

FIG. 1

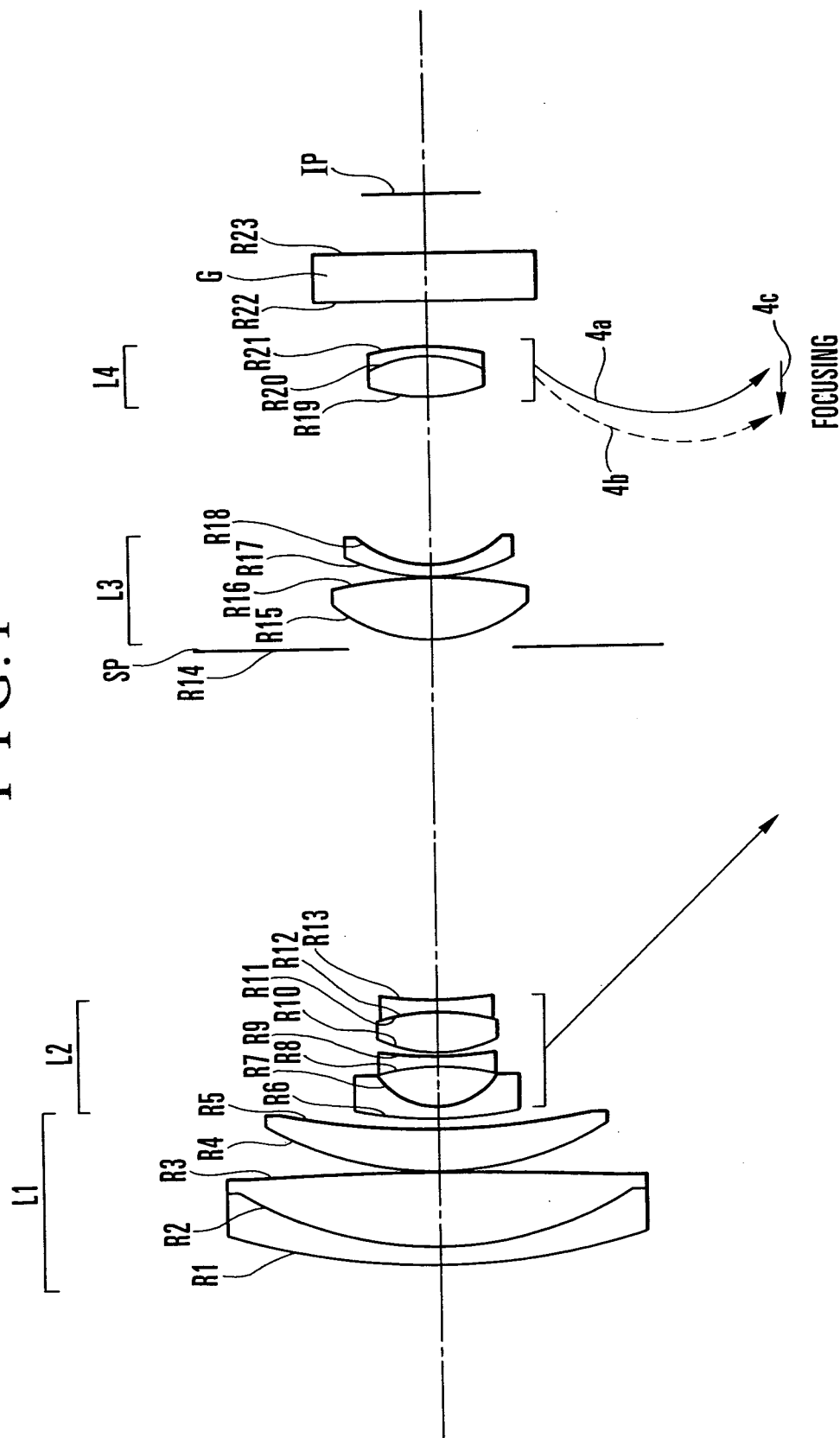


FIG. 2A

FIG. 2B

FIG. 2C

FIG. 2D

FNO / 1.65

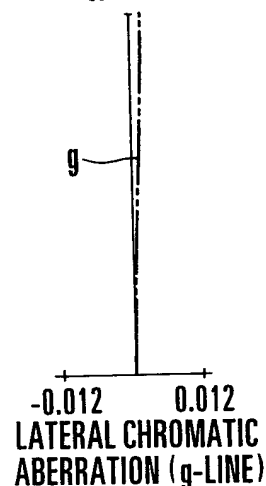
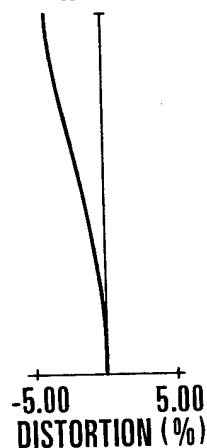
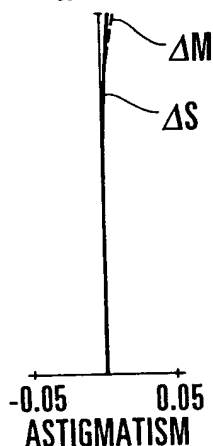
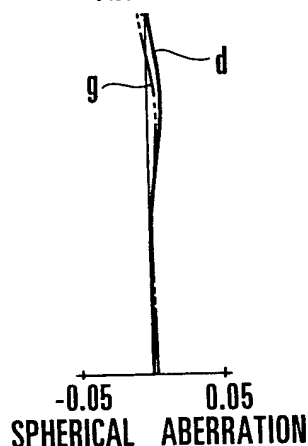
 $\omega = 28.8^\circ$
$$\omega = 28.8^\circ$$
 $\omega = 28.8^\circ$ 

FIG. 3A

FIG. 3B

FIG. 3C

FIG. 3D

FNO / 2.44

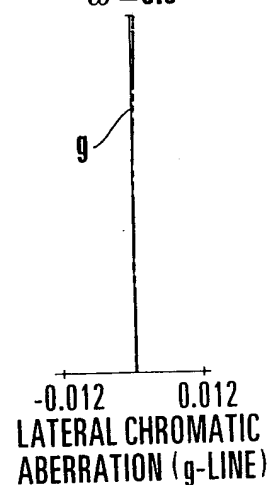
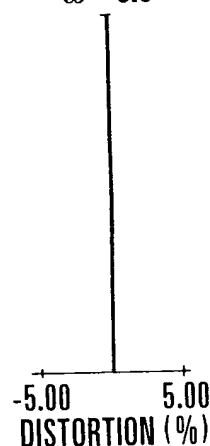
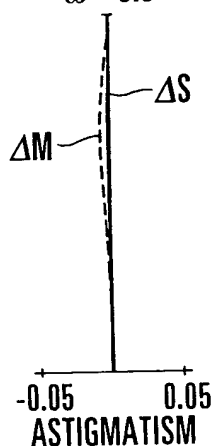
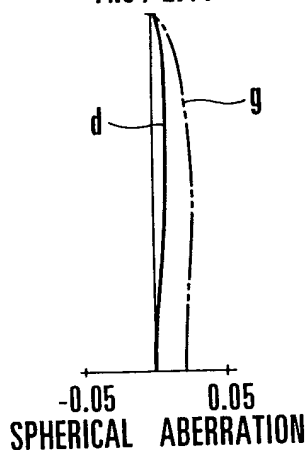
 $\omega = 3.5^\circ$ $\omega = 3.5^\circ$ $\omega = 3.5^\circ$ 

FIG. 4A

FIG. 4B

FIG. 4C

FIG. 4D

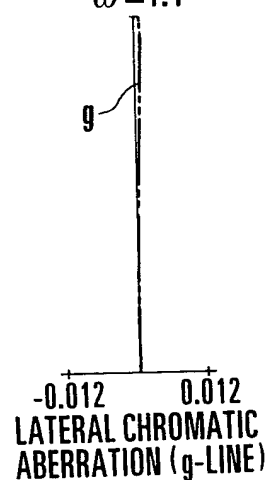
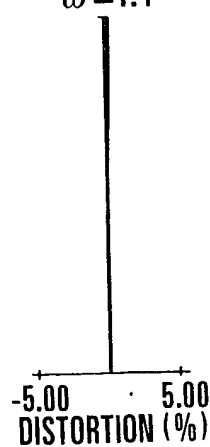
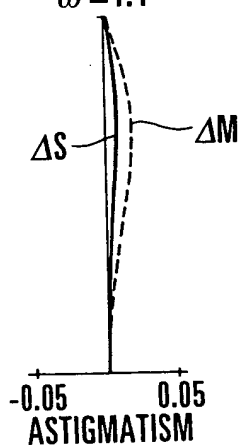
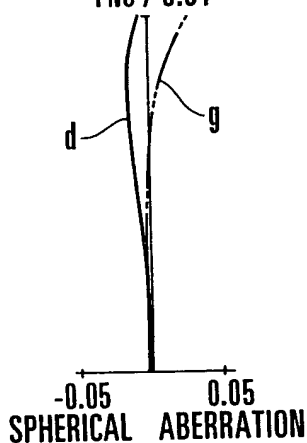
FNO / 3.91 $\omega = 1.4^\circ$ $\omega = 1.4^\circ$ $\omega = 1.4^\circ$ 

FIG. 5

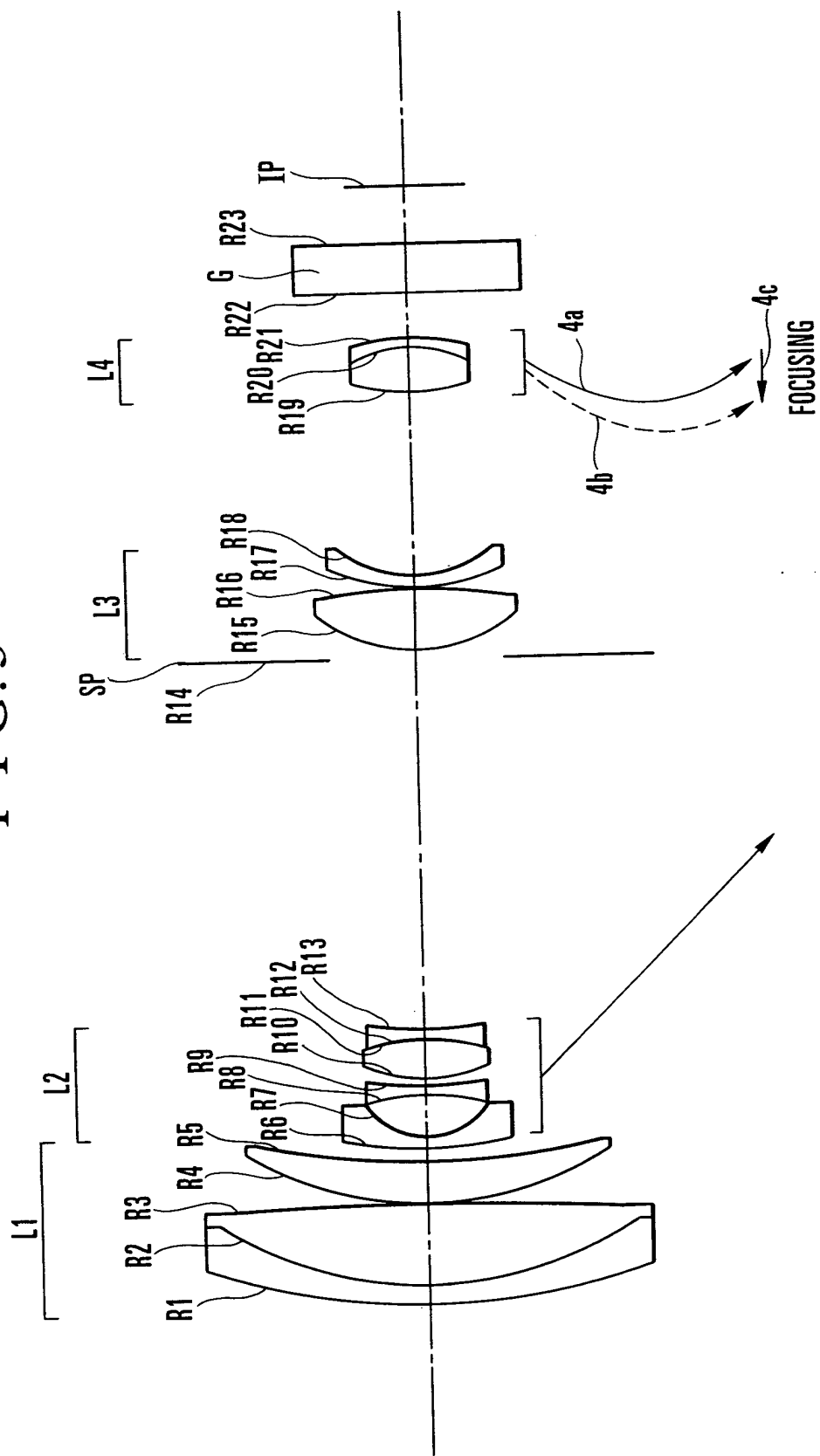


FIG. 6A $FNo / 1.65$
SPHERICAL ABERRATION

FIG. 6B $\omega = 28.9^\circ$
ASTIGMATISM

FIG. 6C $\omega = 28.9^\circ$
DISTORTION (%)

FIG. 6D $\omega = 28.9^\circ$
LATERAL CHROMATIC ABERRATION (g-LINE)

FIG. 7A $FNo / 2.51$
SPHERICAL ABERRATION

FIG. 7B $\omega = 3.3^\circ$
ASTIGMATISM

FIG. 7C $\omega = 3.3^\circ$
DISTORTION (%)

FIG. 7D $\omega = 3.3^\circ$
LATERAL CHROMATIC ABERRATION (g-LINE)

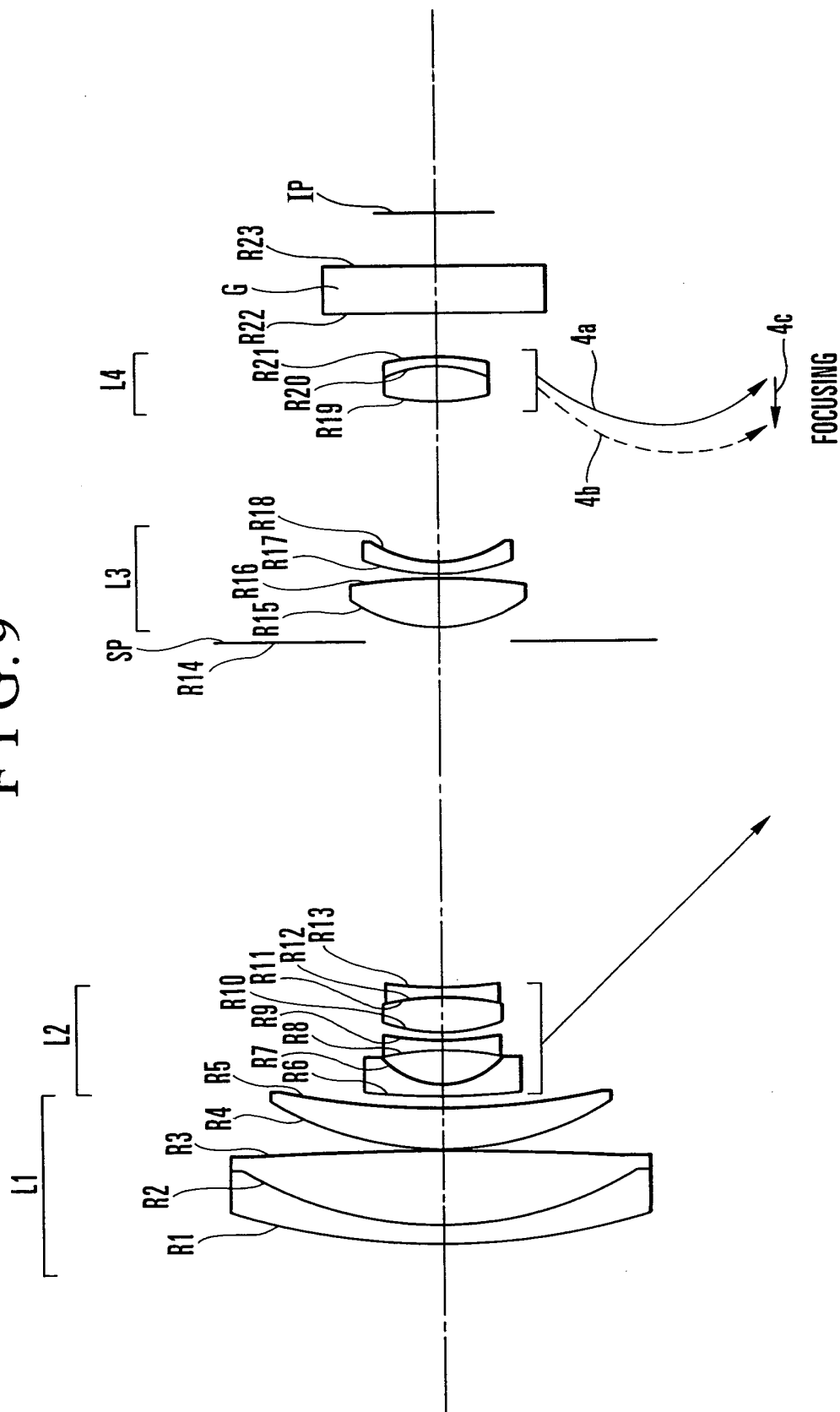
FIG. 8A $FNo / 4.02$
SPHERICAL ABERRATION

FIG. 8B $\omega = 1.3^\circ$
ASTIGMATISM

FIG. 8C $\omega = 1.3^\circ$
DISTORTION (%)

FIG. 8D $\omega = 1.3^\circ$
LATERAL CHROMATIC ABERRATION (g-LINE)

FIG. 9



FNO / 1.85

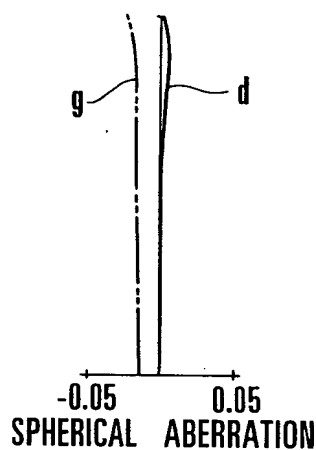


FIG. 10B

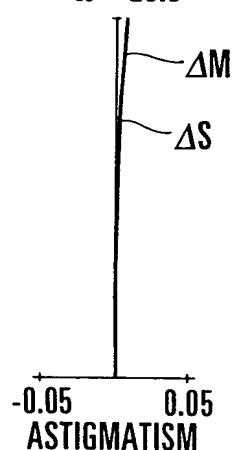
 $\omega = 28.8^\circ$ 

FIG. 10C

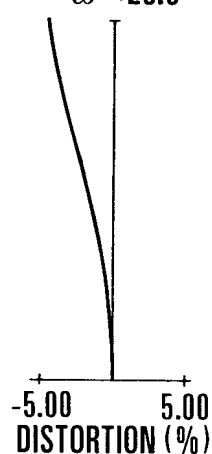
 $\omega = 28.8^\circ$ 

FIG. 10D

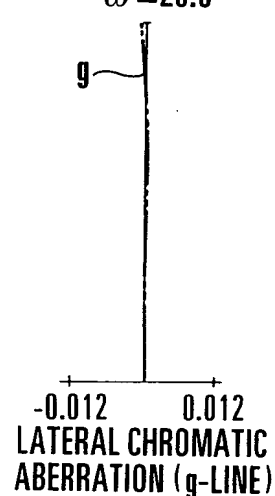
 $\omega = 28.8^\circ$ 

FIG. 11A

FNO / 2.65

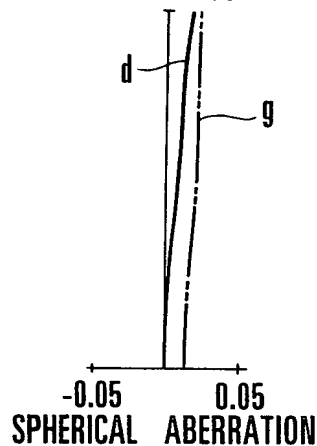


FIG. 11B

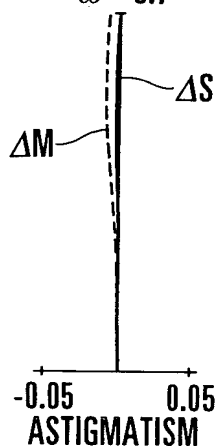
 $\omega = 3.7^\circ$ 

FIG. 11C

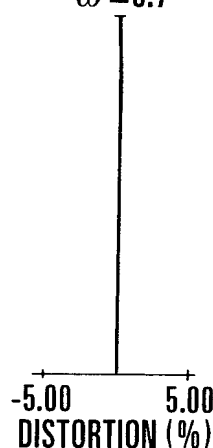
 $\omega = 3.7^\circ$ 

FIG. 11D

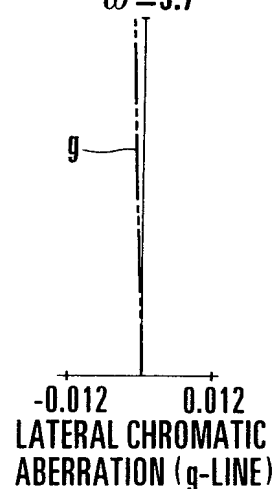
 $\omega = 3.7^\circ$ 

FIG. 12A

FNO / 3.52

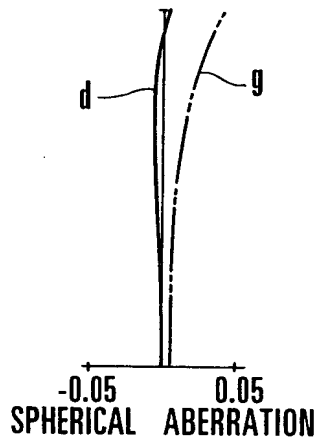


FIG. 12B

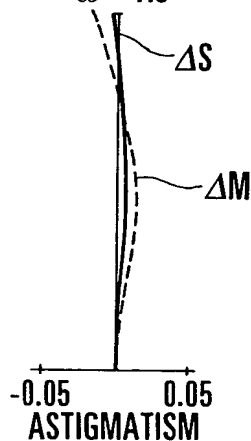
 $\omega = 1.6^\circ$ 

FIG. 12C

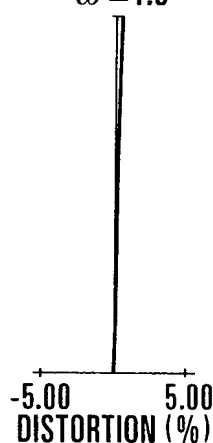
 $\omega = 1.6^\circ$ 

FIG. 12D

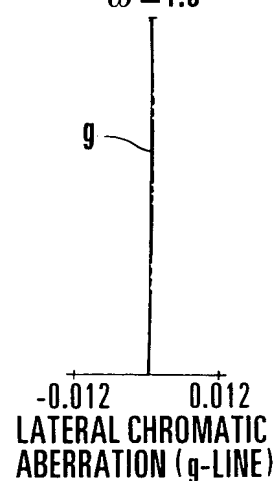
 $\omega = 1.6^\circ$ 

FIG. 14A1 FIG. 14A2 FIG. 14A3 FIG. 14A4

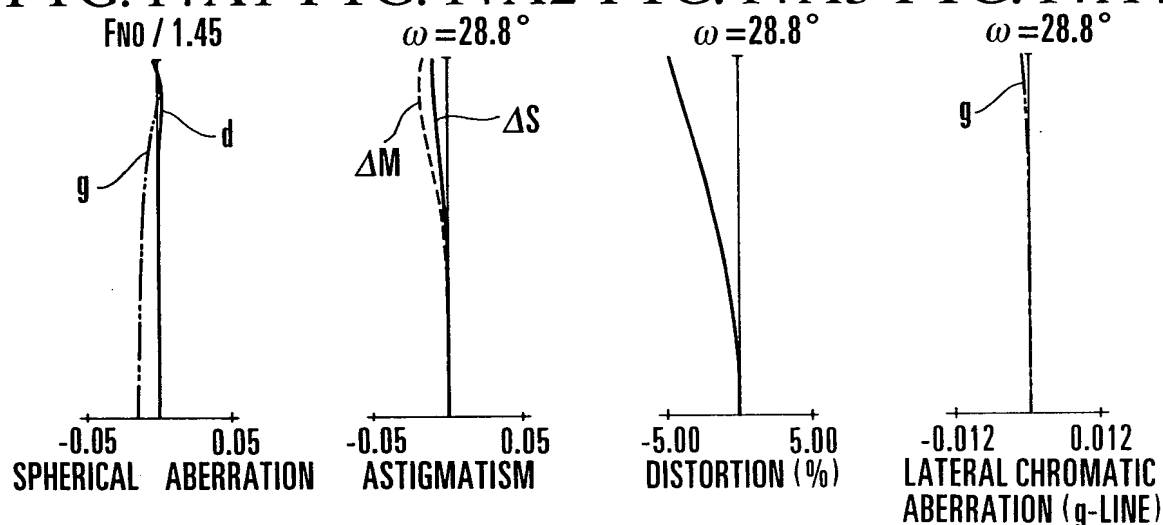


FIG. 14B1 FIG. 14B2 FIG. 14B3 FIG. 14B4

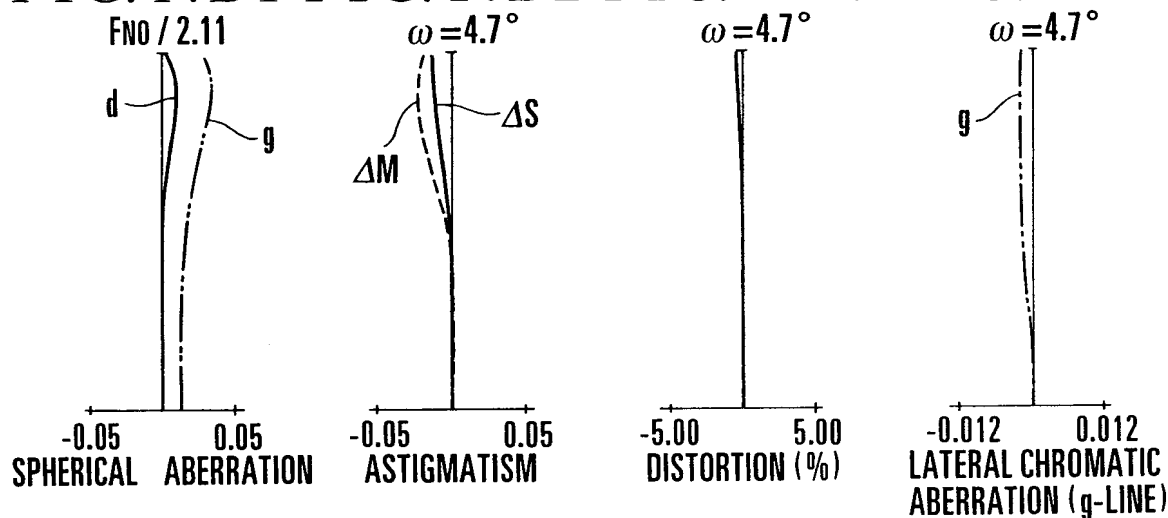


FIG. 14C1 FIG. 14C2 FIG. 14C3 FIG. 14C4

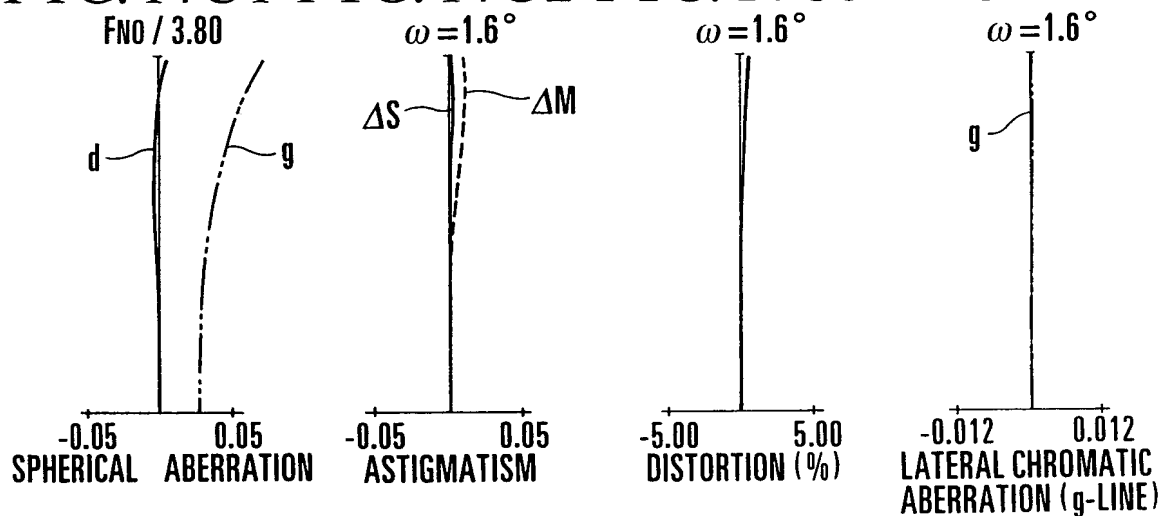
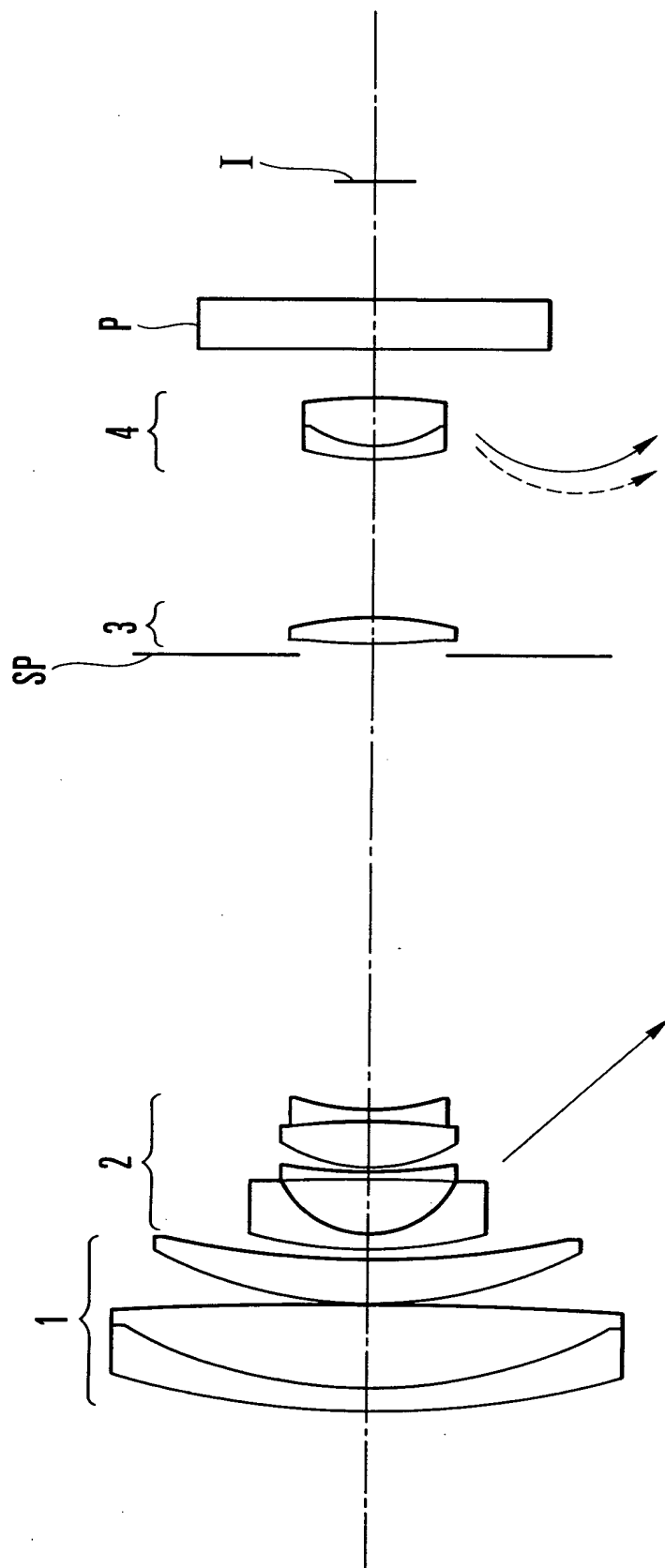


FIG. 15



000001 5718660

FIG. 16A1 FIG. 16A2 FIG. 16A3 FIG. 16A4

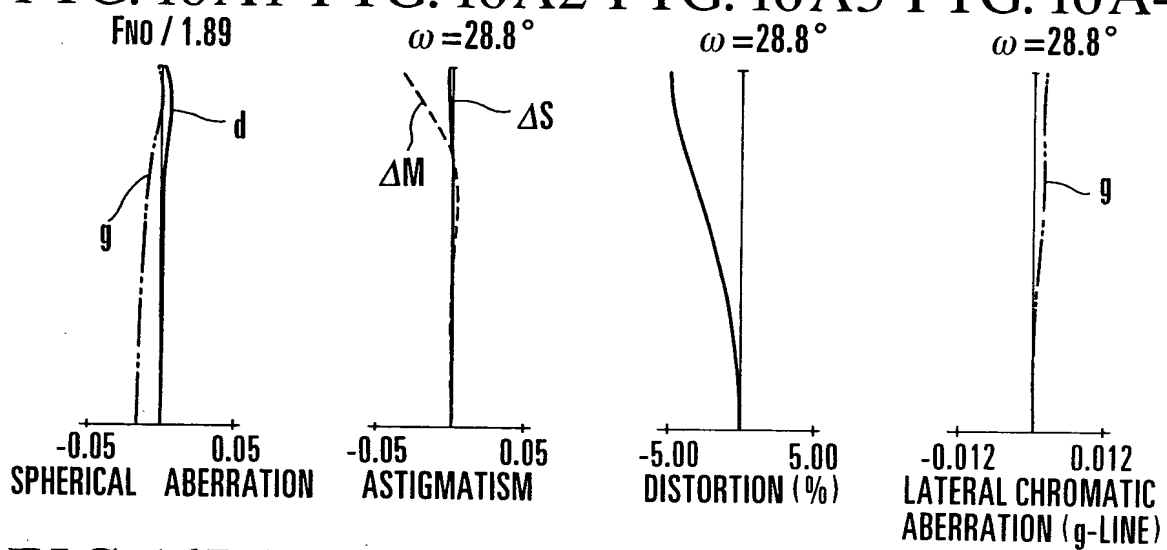


FIG. 16B1 FIG. 16B2 FIG. 16B3 FIG. 16B4

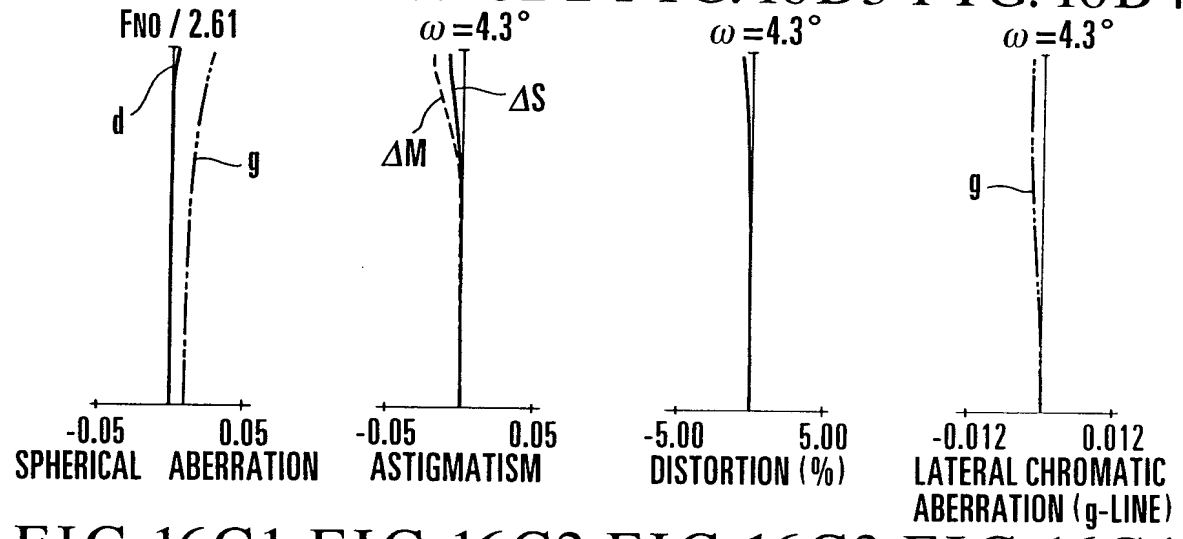


FIG. 16C1 FIG. 16C2 FIG. 16C3 FIG. 16C4

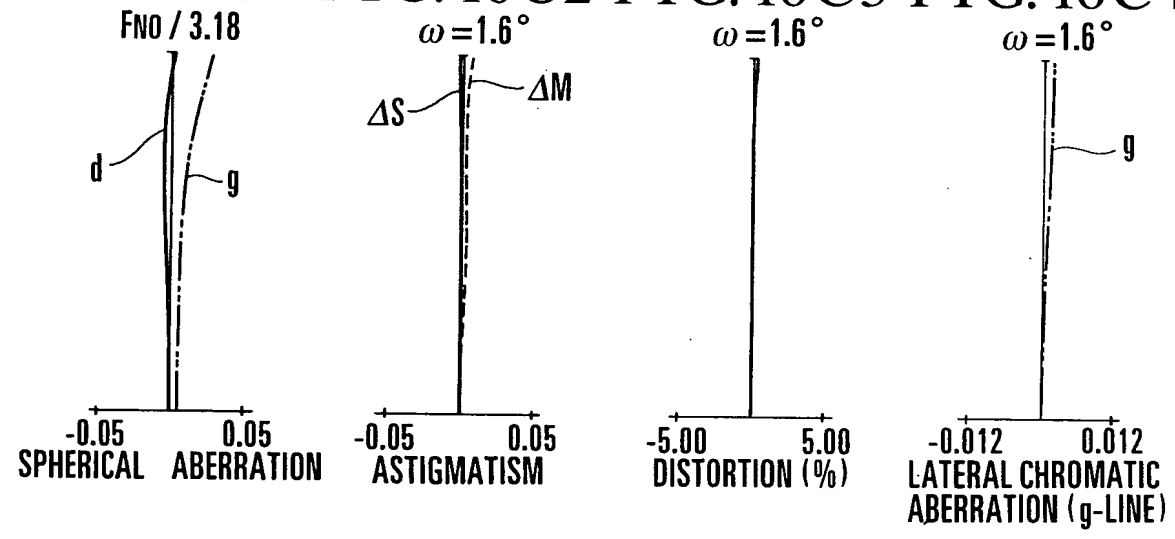


FIG. 17

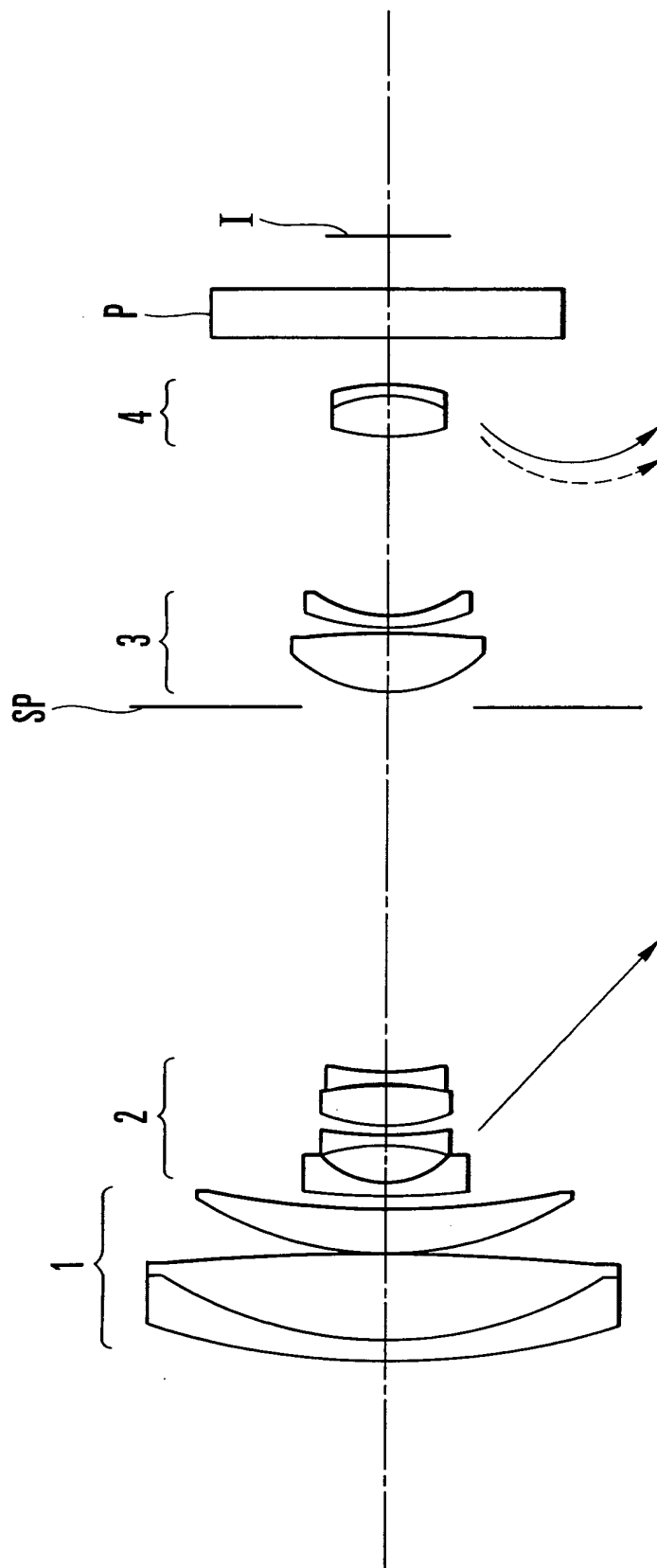


FIG. 18A1 FIG. 18A2 FIG. 18A3 FIG. 18A4

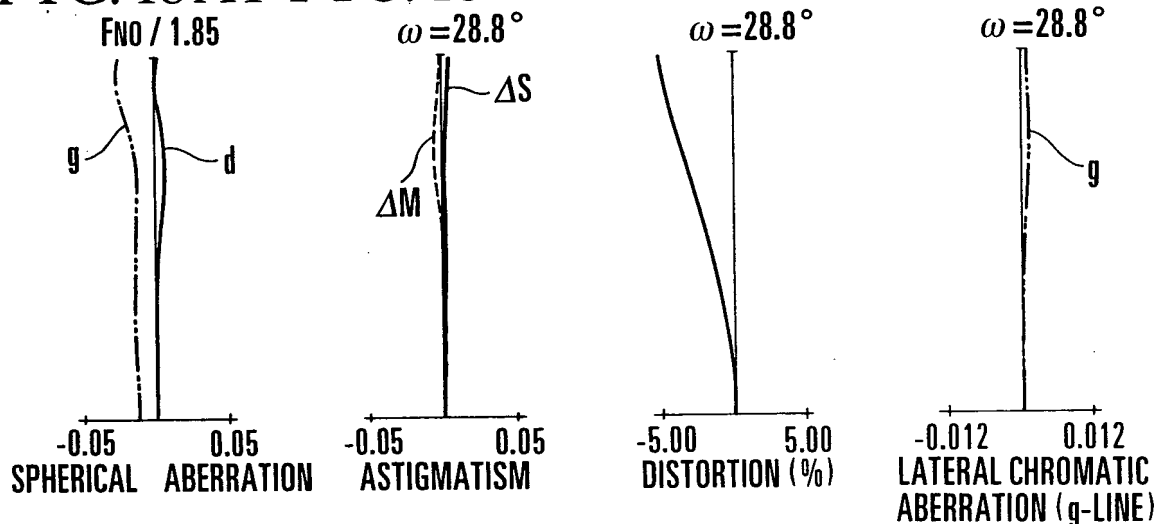


FIG. 18B1 FIG. 18B2 FIG. 18B3 FIG. 18B4

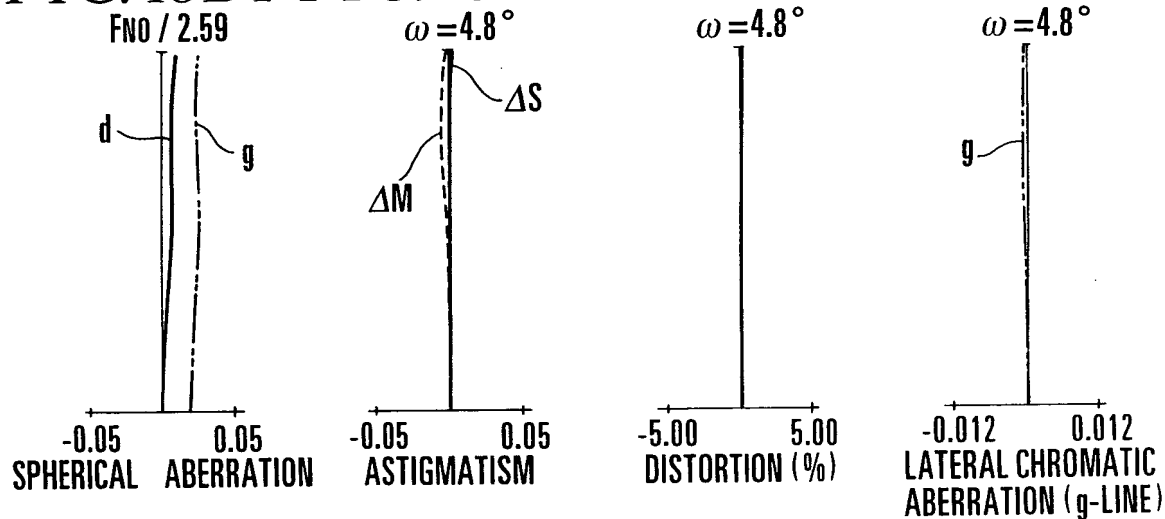
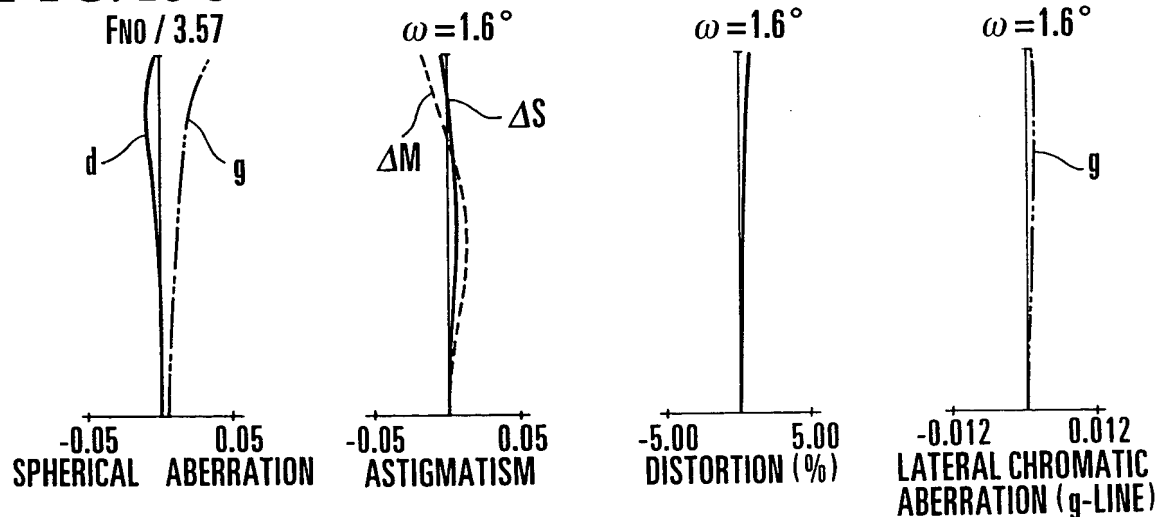


FIG. 18C1 FIG. 18C2 FIG. 18C3 FIG. 18C4



Abstract. We study the asymptotic behavior of the eigenvalues of the Dirac operator $D_{\mathbb{H}^n}$ on the hyperbolic space \mathbb{H}^n with a constant magnetic field. We show that the eigenvalues of $D_{\mathbb{H}^n}$ are asymptotically distributed as a Poisson process with intensity $\frac{1}{2\pi}$ on the real line.

